DOE/ET-53088-95 IFSR #95

CONSTRUCTION OF THREE-DIMENSIONAL VACUUM MAGNETIC FIELDS WITH DENSE NESTED FLUX SURFACES

John R. Cary
Institute for Fusion Studies
The University of Texas at Austin
Austin, TX 78712

May 1983

Construction of Three-Dimensional Vacuum Magnetic Fields with Dense Nested Flux Surfaces

John R. Cary
Institute for Fusion Studies
University of Texas
Austin, Texas 78712

ABSTRACT

Toroidal vacuum magnetic fields are analyzed by the surface of section technique and noncanonical perturbation theory. The surface of section analysis shows that it is easy to find magnetic fields with an outermost flux surface of relatively small aspect ratio. However, as the aspect ratio is decreased, so is the rotational transform of the outermost flux surface. A new method of averaging combined with noncanonical perturbation theory shows that island overlap can account roughly for this loss of rotational transform. Finally, it is shown that one can significantly decrease the stochasticity and island structure by making small modifications to the magnetic field.

I. INTRODUCTION

Magnetic confinement of plasma with scalar pressure is possible only if the associated magnetic fields are integrable, i.e., they lie in nested toroidal flux surfaces.[1] As emphasized by Grad,[2] a rigorous theory of such confinement is possible only if perfect azimuthal symmetry is assumed. (The two other commonly considered cases, which are those of straight and helical symmetry, do not have compact flux surfaces.) However, the case of azimuthal symmetry has a significant drawback. The plasma must have internal toroidal current to produce the rotational transform needed for particle and, hence, plasma confinement. Thus, to have a steady state mode of operation, such a system will require the added complication of a noninductive current drive.

In the stellarator concept,[3,4] the problem of current drive is absent. The necessary rotational transform is produced by external coils. Instead, one faces the difficulty of analyzing even vacuum magnetic fields that do not have a dense set of nested flux surfaces. Indeed, early magnetic field configurations[5] had far from a dense set of nested flux surfaces; large islands and stochastic regions were present. In later designs[6,7] large islands and stochastic regions were absent, but it was not known whether the ultimate field had been obtained, or whether these fields could have been significantly improved by slightly modifying the coil winding law.

In this paper a method for systematically improving the flux surface structure of vacuum magnetic fields is presented. This method is applied to magnetic fields containing a single toroidal harmonic.

It is found that the addition of small amounts of nearby toroidal harmonics can significantly improve the flux surface structure.

To illustrate the nature of typical toroidal magnetic fields, Sec. II contains a study of the flux surface structure obtainable from a magnetic field composed of a purely toroidal field and a single toroidal harmonic. It is shown that variation of the toroidal harmonic amplitude allows one to obtain essentially any aspect ratio, a, for the outermost flux surface. However, as the aspect ratio is decreased, the rotational transform ι_f of the final or outermost flux surface decreases. Thus, the effect of toroidicity is to produce a constraining relationship $\iota_f(a)$ between the final rotational transform and the aspect ratio.

The cause of this constraint is the stochasticity induced by the overlap of islands produced by toroidal effects. In Sec. III it is shown how this effect can be analyzed by a recently developed[8,9] noncanonical perturbation method for Hamiltonian systems. This method relies on the variational form of field-line flow expressed in terms of the covariant components of the vector potential. A new averaging procedure is used to find approximate flux surface and rotational transform values. Then, the perturbation method is used to calculate the locations and widths of the islands.

The perturbation calculation indicates that stochasticity and island structure could be substantially reduced by the addition of other toroidal harmonics chosen to cancel the resonance amplitudes.[10] This causes the islands to vanish through first order. This method is applied in Sec. IV to the magnetic field containing a single toroidal harmonic to find the amplitude of the additional harmonics needed to

decrease stochasticity. The surface of section method is then used to verify that the new fields are substantial improvements over the old fields.

II. STATEMENT OF THE PROBLEM

A precise mathematical question can be asked: All vacuum magnetic fields regular at the toroidal axis, $\xi=0$ (see Appendix B and Fig. 1), can be written as the gradient of a magnetic potential of the form (B1). Can one find a particular set of coefficients such that the magnetic field given by Eq. (B1) has rotational transform and a dense set of flux surfaces?

The physical question, one that might be asked by a designer of stellarator coils, is much less precise. Fabrication errors prevent one from ever obtaining a precisely integrable system. So, the designer would like to know, instead, how close one can get to integrability given the inherent imprecision of the physical world, or whether current designs can be improved to bring them closer to integrability. To answer these questions, one must have a measure of integrability.

A. Typical Toroidal Fields

To illustrate the extent of integrability it is useful to examine typical toroidal fields. As a model of a typical toroidal field, we choose all of the coefficients $\alpha_{\ell m}$ in the magnetic potential (B1) to vanish except α_{ℓ_0,m_0} and $\alpha_{-\ell_0,-m_0}$. Such a magnetic potential contains the dominant terms of the field produced by helical windings on a toroidal surface.

To examine the flux surfaces of a given field, we use the method of surface of section. In this method, one considers the map of the R-Z plane obtained by following a field line through a single field period. (For the previously mentioned case, one field period is $\Delta\phi = 2\pi/m_0$.) If the iterates of the field-line map lie on a curve, then the field lines lie on a surface.

Figure 2 is a surface of section for the case $\ell_0 = 3$, $m_0 = 7$, $\mathrm{Re}(\alpha_{3,7}) = \mathrm{Re}(\alpha_{-3,-7}) = -7 \times 10^{-5}$, and $\mathrm{Im}(\alpha_{3,7}) = \mathrm{Im}(\alpha_{-3,-7}) = 0$. At the center ($R=R_0$, $Z=0$) is a fixed point of the map corresponding to a closed field line. As one considers initial conditions farther from the center, one finds basically good flux surfaces until one begins outside the outermost flux surface shown. Such magnetic lines move rapidly outward from the vicinity of the last closed flux surface. We define the aspect ratio via $a \equiv 1/\bar{\xi}_f$, where $\bar{\xi}_f$ is the mean value of ξ for the final or outermost flux surface. For the case of Fig. 2 we have $a = 9.2$.

The rotational transform of a field line is defined by the formula,

$$\iota \equiv \lim_{\Delta\phi\to\infty} \Delta\eta/\Delta\phi \ , \tag{1}$$

provided the magnetic axis is at $\xi=0$. For later use we also define the rotational transform per field period $\omega \equiv \iota/m_0$. In the case of Fig. 2, the rotational transform vanishes as one approaches the magnetic axis. For the outermost surface shown in Fig. 2, the rotational transform is $\iota_f = -0.832$.

This surface of section looks remarkably clean when compared with those of other nonintegrable maps. (See, for example, Ref. 11, Fig. 1.) On the scale of Fig. 2, islands and stochastic regions are hard to detect. However, they do show up upon closer examination, especially in the vicinity of the final flux surface. A typical relative extent of the largest island is $\Delta\xi/\bar{\xi}_f = 2\%$.

Decreasing the toroidal harmonic amplitude yields a magnetic field with a smaller aspect ratio. Figure 3 is the surface of section for the case $\mathrm{Re}(\alpha_{3,7}) = \mathrm{Re}(\alpha_{-3,-7}) = 3.5 \times 10^{-5}$ and $\mathrm{Im}(\alpha_{3,7}) = \mathrm{Im}(\alpha_{-3,-7}) = 0$. In this case the aspect ratio is approximately 5.7. The final rotational transform value is $\iota_f = -0.643$. Figure 4 is the surface of section for the case $\mathrm{Re}(\alpha_{3,7}) = -1 \times 10^{-5}$ and $\mathrm{Im}(\alpha_{3,7}) = 0$. Now the aspect ratio is approximately a = 3.6, and the final rotational transform is $\iota_f = -0.359$.

This study shows that obtaining small aspect ratio flux surfaces is easy, but that one simultaneously loses rotational transform if one keeps the basic winding law, i.e., the ℓ and m numbers, fixed. One expects particle orbits and stability to improve with rotational transform. Hence, one would like to know whether one can restore the rotational transform while retaining the same aspect ratio and basic winding law.

B. Exactly Integrable Systems

The extent to which rotational transform might be restored can be determined by examining the well-known[4] helically symmetric vacuum magnetic fields with magnetic potential

$$\Phi = IZ + \sum_{\ell=1}^{\infty} (b_\ell/\alpha) I_\ell(\ell\alpha R)\sin(\ell\phi - \ell\alpha Z - \ell\phi_\ell) \ . \qquad (2)$$

The corresponding field lines stay on surfaces of constant

$$\Psi \equiv \frac{1}{2}\,\alpha I R^2 - \sum_{\ell=1}^{\infty} (b_\ell/\alpha) I_\ell'(\ell\alpha R)\cos(\ell\phi - \ell\alpha Z - \ell\phi_\ell)\ , \tag{3}$$

for arbitrary values of α, I, b_ℓ, and ϕ_ℓ. Of course, these surfaces are not compact.

For these fields one can precisely define the commonly used term ℓ-number to be the symmetry number of the flux function Ψ. For a system with ℓ-number ℓ_0, the flux function Ψ is unchanged by the rotation $\phi \to \phi + 2\pi/\ell_0$. One can see from Eq. (3) that ℓ_0 is the largest common divisor of the ℓ-values for which b_ℓ is nonzero. [There is no such precise definition of the ℓ-number of the general toroidal fields of Eq. (B1) since all harmonics of η are present for any nontrivial solution of the form (B1).] One can further see that the flux function Ψ is periodic with periodicity length $L = 2\pi/(\ell_0\alpha)$.

These fields have been studied in detail. (See, for example, Ref. 4, Fig. 2 for contour plots of Ψ.) In the case of an $\ell_0 = 3$ system, a cross-sectional contour plot of Ψ shows a central o-point, where Ψ has a relative minimum, and three (because $\ell_0 = 3$) x-points, which are saddle points of Ψ. The separatrix is the curve connecting the three-x-points. Field lines outside the separatrix are not confined. They eventually reach arbitrarily large values of R. The helical symmetry implies that the flux surfaces rotate through an angle $\Delta\phi = 2\pi/\ell_0$ in one periodicity length.

The field lines that pass through the x-points and o-points are closed. The field line that passes through the o-point stays at R=0. The field line passing through the x-point rotates with the flux

surfaces, and, hence, the rotational transform per field period at the separatrix is $\omega_s = \Delta\phi/2\pi = 1/\ell_0$.

It is therefore expected that the rotational transform at the separatrix of an integrable toroidal field would be $\iota_s = -m_0/\ell_0$. For the cases discussed in Sec. IIA, $m_0/\ell_0 = 2.333$. Yet we found $\iota_f = -0.832$ even for an aspect ratio of 9.2. We conclude that toroidal effects cause typical stellarator fields to lose a significant amount of rotational transform.

III. ANALYSIS OF STOCHASTICITY

A standard method[12] of analyzing stochasticity in nearly integrable Hamiltonian systems is to analyze first the integrable system, then to determine how perturbations move the system away from integrability. A similar method has recently been developed[8,9] for understanding noncanical Hamiltonian mechanics, in particular the problem of magnetic field line flow. This method will be used throughout this section. To apply this method one must first find a nearby integrable system. This is accomplished by an averaging technique. (This is not the method of averaging of Greene and Johnson[13].) Once the averaged fields are throughly understood, the effect of the remainder fields is obtained by a perturbation calculation.

A. Averaging

The averaging technique employed here is based on the variational description of field line flow of Ref. 9, Eq. (3), in which the equations for the trajectory $x^i(\lambda)$ in an arbitrary coordinate system are found by requiring the variation of the flux to vanish:

$$\delta \int A_i(x) \frac{dx^i}{d\lambda} d\lambda = 0. \tag{4}$$

In this equation, the A_i are the covariant components of the vector potential. That is, the cartesian representation of A is

$$A = A_1 \nabla x^1 + A_2 \nabla x^2 + A_3 \nabla x^3 .$$

For the case of Sec IIA, the covariant components are

$$A_i = A_i^T(\xi,\eta) + [\alpha_{\ell_0 m_0} A_i^{\ell_0 m_0}(\xi,\eta,\phi) + c.c.] \tag{5}$$

where A_i^T and $A_i^{\ell_0 m_0}$ are given by Appendix C.

In the variation (4), λ is arbitrary parameter. One can take it to be one of the coordinates. If the coordinate x^3 is chosen, one finds the flow equations,

$$\frac{dx^1}{dx^3} = \frac{B_{23}}{B_{12}} \tag{6a}$$

and

$$\frac{dx^2}{dx^3} = \frac{B_{31}}{B_{12}} , \tag{6b}$$

where B_{ij} are the components of the magnetic field in the Clebsch or two-form representation:

$$B = B_{12}\nabla x^1 \times \nabla x^2 + B_{23}\nabla x^2 \times \nabla x^3 + B_{31}\nabla x^3 \times \nabla x^1 . \tag{7}$$

An important aspect of this formulation is the presence of Noether's theorem, which implies the existence of an invariant, if the covariant components of the vector potential are independent of one of the coordinates. This cannot be applied directly to the expression (5), in which there is dependence on all three coordinates. However, in the limit $\xi \to 0$, the primary dependence of the vector potential components is on ξ and the helical angle $h \equiv \ell_0\eta - m_0\phi$. For this reason the averaged components,

$$\bar{A}_i(\xi,h) \equiv \frac{1}{2\pi}\int_0^{2\pi} d\eta\, A_i(\xi,\eta,\phi = (h-\ell_0\eta)/m_0) , \tag{8}$$

are introduced. In the limit of small ξ, the averaged vector potential differs little from the actual vector potential. The calculation of these averaged fields is discussed in Appendix D.

The averaged vector potential has the form

$$\bar{A} = \bar{A}_\xi(\xi,h)\nabla\xi + \bar{A}_\eta(\xi,h)\nabla\eta + \bar{A}_\phi(\xi,h)\nabla\phi .$$

Thus, it is natural to use the new variable h in place of ϕ. To find

the covariant components of A in the (ξ,η,h) system, one uses the relation $\nabla\phi = \nabla h/m_0 - \ell_0\nabla\eta/m_0$ to obtain

$$\bar{A} = \bar{A}_\xi(\xi,h)\nabla\xi + (\bar{A}_\eta - \ell_0\bar{A}_\phi/m_0)\nabla\eta + (\bar{A}_\phi/m_0)\nabla h \ . \tag{9}$$

(Note that the η-component of A has changed even though η has not changed.) In this coordinate system the covariant components of the vector potential do not depend on the coordinate η. Hence,

$$\psi \equiv \bar{A}_\eta(\xi,h) - \ell_0\bar{A}_\phi(\xi,\psi)/m_0 \ , \tag{10}$$

is an invariant of the flow of $\bar{A}$. While $\bar{A}$ has an exact invariant, it is no longer a vacuum field. This property was destroyed by the process of averaging.

The usefulness of the method of averaging follows from the following line of reasoning. For small values of ξ, the averaged vector potentials are close to the actual vector potential. Therefore, the exact invariant of the approximate flow is an approximate invariant of the exact flow. For the particular field of Eq. (5), this approximate invariant is given by

$$\psi = \bar{A}_\eta^T + \left[\alpha_{\ell_0 m_0}\bar{A}_\eta^{\ell_0 m_0}(\xi,h) + c.c\right] \ , \tag{11}$$

for which the $\bar{A}$-functions are defined in Appendix D.

The results of this line of reasoning are shown in Figs. 5 and 6. In these figures we have overlayed the contours of ψ as given by Eq. (11) on the surfaces of section of Figs. 3 and 4. One can see that a field line does stay close to a contour of ψ, especially for small ξ.

Significant deviations are observed only for the outermost flux surfaces.

B. Analysis of Averaged Fields

An analysis of the averaged fields yields their flux coordinates and rotational transform. Later calculations are simplified by use of the flux coordinates, in which the averaged flow is trivial. The rotational transform profiles are needed to determine the location of resonances.

The first step in finding the flux coordinates is to use the invariant ψ as one of the coordinates. In the present case we eliminate ξ in favor of ψ. This transformation is nonsingular only if the magnetic axis remains at $\xi=0$. For simplicity we assume this to be the case. To transform the vector potential we need the inverse transformation, $\xi = f(\psi,h)$. In the (ψ,η,h) coordinate system, the vector potential is

$$\bar{A} = \bar{A}_\xi(f(\psi,h),h)\,\frac{\partial f}{\partial \psi}\,\nabla\psi + \psi\nabla\eta$$

$$+ \left[\bar{A}_\phi(f(\psi,h),h)/m_0 + \bar{A}_\xi(f(\psi,h),h)\,\frac{\partial f}{\partial h}\right]\nabla h \,. \qquad (12)$$

The curl of this vector potential yields the magnetic field,

$$\bar{B} = \left(\frac{\partial \bar{A}_\xi}{\partial h} - \frac{\partial \bar{A}_\phi}{\partial \xi}/m_0\right)\left(\frac{\partial \psi}{\partial \xi}\right)^{-1} \nabla h \times \nabla\psi + \nabla\psi \times \nabla\eta \,.$$

The next step is to introduce a new angle

$$\theta \equiv \eta - \hat{\eta}(\psi,h) \tag{13}$$

so that in the new coordinate system the averaged magnetic field components do not depend on h. In the new coordinate system, the averaged magnetic field has the form

$$\bar{B} = \left[\left(\frac{\partial \bar{A}_\xi}{\partial h} - \frac{\partial \bar{A}_\phi}{\partial \xi}/m_0\right)\left(\frac{\partial \psi}{\partial \xi}\right)^{-1} + \frac{\partial \hat{\eta}}{\partial h}\right]\nabla h \times \nabla\psi + \nabla\psi \times \nabla\theta \ .$$

Hence, with the definition,

$$\bar{B}_{h\psi}(\psi) \equiv \frac{1}{2\pi}\int_0^{2\pi} dh\left[\frac{\partial \bar{A}_\xi}{\partial h}(f(\psi,h),h) - \frac{\partial \bar{A}_\phi}{\partial \xi}(f(\psi,h),h)/m_0\right]\left[\frac{\partial \psi}{\partial \xi}(f(\psi,h),h)\right]^{-1} \tag{14}$$

and the choice,

$$\hat{\eta}(\psi,h) = \int_0^h dh\left[\bar{B}_{h\psi} - \left(\frac{\partial \bar{A}_\xi}{\partial h} - \frac{\partial \bar{A}_\phi}{\partial \xi}/m_0\right)\left(\frac{\partial \psi}{\partial \xi}\right)^{-1}\right] , \tag{15}$$

the magnetic field can be written in the form

$$\bar{B} = \bar{B}_{h\psi}(\psi)\ \nabla h \times \nabla\psi + \nabla\psi \times \nabla\theta \ . \tag{16}$$

A vector potential corresponding to Eq. (16) is

$$\bar{A} = \bar{A}_h(\psi)\ \nabla h + \psi\nabla\theta \ , \tag{17}$$

with

$$\bar{A}_h(\psi) = -\int_0^{\psi} d\psi \bar{B}_{h\psi}(\psi) \ . \tag{18}$$

In general, this vector potential differs from that of Eq. (12) by a gauge transformation.

In these (flux) coordinates the magnetic flow is given by the simple expressions

$$\frac{d\psi}{dh} = 0 \tag{19a}$$

and

$$\frac{d\theta}{dh} = \bar{B}_{h\psi}(\psi) \ . \tag{19b}$$

As one approaches the separatrix, the integral (14) diverges because $\partial\psi/\partial\xi$ approaches zero at the x-point. Therefore, $\bar{B}_{h\psi}(\psi) \to \infty$ as ψ approaches ψ_s, the value at the separatrix.

The results (19) allow one to find the rotational transform. From the definition (1), we find

$$\iota = \lim_{\Delta\phi\to\infty} \left(\frac{\Delta\eta}{\Delta\phi} = \frac{\Delta\eta}{\Delta h/m_0 - \ell_0\Delta\eta/m_0}\right) = \left(\lim_{\Delta\eta\to\infty} \frac{\Delta h}{m_0\Delta\eta} - \frac{\ell_0}{m_0}\right)^{-1} \ . \tag{20}$$

Then we use the fact that the difference between η and θ is a periodic function to put Eq. (20) into the form

$$\iota = m_0 \bar{B}_{h\psi}(\psi)/(1 - \ell_0 \bar{B}_{h\psi}) \ . \tag{21}$$

At the separatrix, where $\bar{B}_{h\psi}$ diverges, $\iota_s = -m_0/\ell_0$, just as in the integrable case discussed in Sec. IIB.

The rotational transform for the averaged fields of the case of Fig. 2 is shown in Fig. 7. As can be seen in the figure, the rotational transform is linear in ψ for small ψ. Near the separatrix the rotational transform rises sharply to the value $|\iota_s| = 7/3$, which is not shown here.

C. Effect of Perturbations

The total vector potential,

$$A = \bar{A} + \varepsilon \tilde{A} \ , \tag{22}$$

contains the remainder term $\varepsilon\tilde{A}$, which is found by subtracting $\bar{A}$ from A, in addition to the averaged part. (The ε is inserted here merely as a reminder that $\tilde{A}$ is a perturbation. It is set to unity at the end of the calculation.) The effect of the remainder term is analyzed by perturbation theory, which is essentially a search for new coordinates in which the motion is simple.

The ease of describing the unperturbed flow in the coordinates (ψ,θ,h) indicates that it would be useful to transform the perturbation to this coordinate system also. This is accomplished by using the general covariant transformation law. The result is

$$\tilde{A} = \tilde{A}_\psi(\psi,\theta,h)\nabla\psi + \tilde{A}_\theta(\psi,\theta,h)\nabla\theta + \tilde{A}_h(\psi,\theta,h)\nabla h \ , \tag{23}$$

where

$$\tilde{A}_\psi = \tilde{A}_\xi \frac{\partial f}{\partial \psi} + (\tilde{A}_\eta - \ell_0 \tilde{A}_\psi/m) \frac{\partial \hat{\eta}}{\partial \psi} , \tag{24a}$$

$$\tilde{A}_\Theta = \tilde{A}_\eta - \ell_0 \tilde{A}_\phi/m_0 , \tag{24b}$$

and

$$\tilde{A}_h = \tilde{A}_\xi \frac{\partial f}{\partial h} + \tilde{A}_\eta \frac{\partial \hat{\eta}}{\partial h} + \tilde{A}_\phi (1 - \ell_0 \frac{\partial \hat{\eta}}{\partial h})/m_0 . \tag{24c}$$

To determine the effect of perturbations, new coordinates (Ψ,Θ,H) and a gauge transformation, $A \to A+\nabla\hat{s}$, are introduced. The coordinates and gauge transformation are chosen to return the vector potential to flux-coordinate form. One difference between this calculation and that of Ref. 9 is that Lie transforms are not used here.

The coordinate transformation has the form,

$$\psi = \Psi + \varepsilon\tilde{\psi}(\Psi,\Theta,H) \tag{25a}$$

$$\theta = \Theta + \varepsilon\tilde{\theta}(\Psi,\Theta,H) \tag{25b}$$

$$h = H , \tag{25c}$$

in which $\tilde{\psi}$ and $\tilde{\theta}$ must be periodic functions of Θ and H. As discussed in Ref. 9, one of the coordinates, in this case h, may be left unchanged without loss of generality. With this transformation and the gauge function $\hat{s}(\Psi,\Theta,H)$ the transformation becomes

$$A = \Psi\nabla\Theta + \bar{A}_h(\Psi)\nabla H + \varepsilon\Big[\Big(\Psi\frac{\partial\tilde{\theta}}{\partial\Psi} + \tilde{A}_\psi + \frac{\partial\hat{s}}{\partial\Psi}\Big)\nabla\Psi$$

$$+ \Big(\tilde{\psi} + \Psi\frac{\partial\tilde{\theta}}{\partial\Theta} + \tilde{A}_\theta + \frac{\partial\hat{s}}{\partial\Theta}\Big)\nabla\Theta + \Big(\Psi\frac{\partial\tilde{\theta}}{\partial H} + \frac{\partial\bar{A}_h}{\partial\psi}\tilde{\psi} + \tilde{A}_h + \frac{\partial\hat{s}}{\partial H}\Big)\nabla H\Big] + \mathcal{O}(\varepsilon^2) \ . \quad (26)$$

It is important to recognize that the old vector potentials are evaluated at the new coordinates; i.e., the second term on the right-hand side of Eq. (26) is <u>not</u> $\bar{A}_h(\bar{\psi}+\tilde{\psi})\nabla H$.

To preserve the flux coordinate form, $\tilde{\psi}$ and $\tilde{\theta}$ are chosen to leave the Ψ and Θ components of A unchanged. This condition results in the choices,

$$\tilde{\theta} = \tilde{A}_\psi(\Psi,\Theta,H) + \frac{\partial s}{\partial\Psi} \quad (27a)$$

and

$$\tilde{\psi} = -\tilde{A}_\theta(\Psi,\Theta,H) - \frac{\partial s}{\partial\Theta} \ , \quad (27b)$$

where

$$s \equiv \hat{s} + \Psi\tilde{\theta} \ . \quad (27c)$$

At this point we have

$$A = \Psi\nabla\Theta + A_H\nabla H + \mathcal{O}(\varepsilon^2) \ , \quad (28)$$

where

$$A_H = \bar{A}_h(\Psi) + \tilde{A}_h - \frac{\partial \bar{A}_h}{\partial \psi}(\Psi)\tilde{A}_\theta - \frac{\partial s}{\partial H} + \frac{\partial \bar{A}_h}{\partial \psi}(\Psi)\frac{\partial s}{\partial \Theta} \ . \qquad (29)$$

The last step is to choose the gauge function. If the magnetic field perturbations were not disturbing the property of integrability, it would be possible to choose s to reduce A_H to being a function of Ψ alone. To see that this is not generally possible, it is useful to go to the Fourier representation. With the definitions,

$$\tilde{r}_{jk}(\psi) \equiv \frac{1}{(2\pi)^2}\int_0^{2\pi} d\theta \int_0^{2\pi} dh \ e^{-ij\theta - ikh}\left[\tilde{A}_h(\psi,\theta,h) - \frac{\partial \bar{A}_h}{\partial \psi}(\psi)\tilde{A}_\theta(\psi,\theta,h)\right] , \qquad (30)$$

and

$$s_{jk}(\psi) \equiv \frac{1}{(2\pi)^2}\int_0^{2\pi} d\theta \int_0^{2\pi} dh \ e^{-ij\theta - ikh}\ s(\psi,\theta,h) \ , \qquad (31)$$

Eq. (29) can be put into the form

$$A_H(\Psi,\Theta,H) = \bar{A}_h(\Psi) + \sum_{j,k}\left\{\tilde{r}_{jk}(\Psi) + i\left[j\frac{\partial \bar{A}_h}{\partial \psi}(\Psi) - k\right]s_{jk}(\Psi)\right\}e^{ij\Theta + ikH} \ . \qquad (32)$$

It can now be seen that the requirement that $\bar{A}_H$ be a function of Ψ alone leads to the following gauge function choice,

$$s_{jk}(\psi) = i\ \tilde{r}_{jk}(\psi)/\left(k - j\frac{\partial \bar{A}_h}{\partial \psi}\right) \ , \qquad (33)$$

which diverges if there exists a surface ψ_{jk}, such that

$$\frac{\partial \bar{A}_h}{\partial \psi}(\psi_{jk}) = k/j \ , \tag{34}$$

and

$$\tilde{r}_{jk}(\psi_{jk}) \neq 0 \ . \tag{35}$$

In general, the rational surfaces ψ_{jk} are dense, and, hence, no continuous gauge function s can be found. Instead, one finds that rational surfaces break up into islands. The calculation of island structure has been carried out in detail in Ref. 9, and will not be repeated here. We simply quote the result

$$\Delta\psi_{jk} = |8\tilde{r}_{jk}(\psi_{jk})/\frac{\partial^2 \bar{A}_h}{\partial \psi^2}(\psi_{jk})|^{1/2} \ , \tag{36}$$

for the half-width of the island.

The resonance widths and locations for several islands were calculated numerically. The results for the case of Fig. 3 are tabulated in Table I. As one can see, the (3,1) and (4,1) islands nearly overlap. Given the known[12] optimistic errors typical of the overlap criterion, one would predict $|\iota_f| \lesssim 0.88$ on the basis of Table I. This agrees with the numerical result $|\iota_f| = 0.64$ obtained in Sec. IIA.

IV. ELIMINATION OF STOCHASTICITY

The analysis of Sec. III leads to the following observation. If one could arrange for $\tilde{r}_{jk}(\psi_{jk})$ to vanish, then the transformation (25a) would give a new approximate flux invariant valid to $\mathcal{O}(\varepsilon^2)$. This implies that the islands and stochastic regions would be smaller. In this section it is shown how to satisfy the condition $\tilde{r}_{jk}(\psi_{jk}) = 0$.

A. Effects of Additional Fields

If other harmonics of smaller amplitude are added to the basic single-harmonic field, the vector potential becomes

$$A = \bar{A} + \varepsilon\tilde{A} + \varepsilon \sum_{(\ell,m)\neq(\ell_0,m_0)} \alpha_{\ell m} A^{\ell m} . \tag{37}$$

The factor ε preceding the summation sign indicates that the amplitudes of these additional fields are small. This is consistent since they will be chosen to cancel small resonances produced by $\varepsilon\tilde{A}$.

With these additional fields the analysis of Sec. IIIC is only slightly modified. The same transformation law (24) can be used to obtain the components of $A^{\ell m}$ in the (ψ,θ,h) coordinate system. The equation analogous to (32) is

$$A_H(\Psi,\Theta,H) = \bar{A}_h(\Psi) + \sum_{j,k} \{\tilde{r}_{jk}(\Psi) + i\left[j \frac{\partial \bar{A}_h}{\partial \psi}(\Psi) - k\right] s_{jk} + \sum_{(\ell,m)\neq(\ell_0,m_0)} \alpha_{\ell m} r_{jk}^{\ell m}(\Psi)\} e^{ij\Theta + ikH} , \tag{38}$$

where

$$r_{jk}^{\ell m}(\psi) \equiv \frac{1}{(2\pi)^2}\int_0^{2\pi} d\theta \int_0^{2\pi} dh e^{-ij\theta - ikh}\left[A_h^{\ell m}(\psi,\theta,h) - \frac{\partial \bar{A}_h}{\partial \psi}(\psi) A_\theta^{\ell m}(\psi,\theta,h)\right] . \quad (39)$$

In general, the quantities $r_{00}^{\ell m}(\psi)$ do not vanish. These terms produce modifications of the rotational transform profile.

The more important consequence is the addition of the $(j,k) \neq (0,0)$ terms. If one can choose the amplitudes $\alpha_{\ell m}$ such that

$$\tilde{r}_{jk}(\psi_{jk}) + \sum_{(\ell,m)\neq(\ell_0,m_0)} \alpha_{\ell m} r_{jk}^{\ell m}(\psi_{jk}) = 0 \quad (40)$$

for all (j,k) such that $0 < \psi_{jk} < \psi_s$, then the transformation (25a), corrected by adding in the other harmonics, yields an approximate invariant valid to higher order.

Equation (40) is an infinite-order matrix equation. Whether it has no solution, a unique solution, or many solutions depends on the space of allowable solutions. This space should at least include differentiable vector potentials. This difficult mathematical question will not be further discussed here. Instead, the results of a numerical calculation will be given.

B. Selection of Cancelling Fields

A numerical solution to Eq. (40) is necessarily limited to a finite number of resonances and a finite number of amplitudes. Upon requiring the number of allowed amplitudes to equal the number of resonances, Eq. (40) reduces to a finite-order matrix equation which can be solved by elementary means.

However, now one must decide which resonances to consider and which amplitudes to use. It is possible that the addition of a harmonic to remove one resonance causes other resonances to increase in size. To prevent this one must determine the harmonic that has the greatest effect on a given resonance.

To determine which resonances are large, one notes that the terms in $\tilde{A}$ have the form

$$a(\xi)\cos[(\ell_0+\Delta\ell)\eta+m_0\phi] = a(f(\psi,h))\cos(h+\Delta\ell\eta)$$

$$= a(f(\psi,h))\cos(h+\Delta\ell\hat{\eta}(\psi,h)+\Delta\ell\theta) \ . \quad (41)$$

The largest terms will be those with $|\Delta\ell| = 1$. In general, the relative magnitude of a term of form (41) will be of order $\xi^{|\Delta\ell|}$. The Fourier amplitudes of a term of form (41) are nonzero only for $j = \Delta\ell$. No restriction on the k-values is implied by Eq. (41), but the fundamental (k=1) amplitude is expected to be the largest. To summarize, the dominant resonance should satisfy $|j| = |k| = 1$.

The necessary additional fields should have the same periodicity as the original system. This implies that it will be necessary to add fields with vector potential components of the form,

$$b(\xi)\cos(\ell\eta+nm_0\phi) = b(f(\psi,h))\cos[(\ell-n\ell_0)\eta+nh] \ . \quad (42)$$

With the same reasoning as before, one notes that the dominant Fourier amplitude of this term has $j = (\ell-n\ell_0)$ and $k=n$. Thus, to cancel the (j,k) amplitude we want to add some of the $(\ell=j+k\ell_0,\ m=km_0)$ toroidal harmonic.

C. Numerical Results

The numerical methods used to calculate the quantities $\tilde{r}_{jk}(\psi_{jk})$ and $r^{\ell m}_{jk}(\psi_{jk})$ were relatively straightforward. Analytical formulas for $A,\bar{A},\tilde{A}$, and $\psi(\xi,h)$ are known. The inversion $f(\psi,h)$ was found numerically via Newton's method. The Fourier integrals of Eqs. (30) and (39) were calculated by the trapezoidal rule using a (θ,h) grid of roughly 100 × 100 points. Additional points were added in the vicinity of the x-point where the integrand can become highly peaked. The special functions $U_{\ell m}(\xi)$ were evaluated by a code written by Robert Pexton[14] and modified by Joe Sedlak.[15]

This method was applied in detail to the field which produced Fig. 3. In the first attempt, the amplitudes of the (ℓ=4,5,...,10;m=7) fields needed to cancel the (j=1,2,...,7;k=1) resonances were calculated. The reason for this choice is that the initial study had shown that the flux surfaces satisfying $|\tau| > 0.671$ had been destroyed. It was felt that restoration of these surfaces would require elimination of islands with (j,k) values corresponding to $0.671 < m/\ell < 7/3$ and $m=m_0$. The resulting amplitudes are shown in Table II.

These fields were added to the original field. The surface of section of the total field is shown in Fig. 8. The sharper corners of the outer flux surface, when compared with that of Fig. 3, indicate that surfaces close to the separatrix have been restored. A detailed examination of this new field found no significant internal islands. Furthermore, one notes that the new flux surfaces look more nearly symmetric in the sense of a simple rotation by angle of $\pi/3$ of the R-Z plane about the magnetic axis ξ=0. In addition, the magnitude of the

final value of rotational transform has been significantly increased to $|\iota_f| = 0.926$. This is an increase of 38%.

It may seem surprising that the volume enclosed by the outermost flux surface has changed little from the original system of Fig. 3. This can be understood on the basis of Fig. 7, which shows that near the separatrix a large change in rotational transform is accompanied by a small change in enclosed flux. This is not a drawback. To obtain a smaller aspect ratio final system, one simply begins with a smaller aspect ratio initial system. Indeed, by comparing the case of Fig. 8 with that of Fig. 1, one notes that the new system has a 60% smaller aspect ratio and an 11% increase in rotational transform of the outer flux surface.

To determine the sensitivity of these results, a surface of section analysis was made for the case of Table II with the (4,7) amplitude increased by 6%. This caused the rotational transform of the outermost flux surface to decrease only slightly from 0.926 to 0.908. Another surface of section analysis for the case of Table II with all of the amplitudes for $\ell \geq 6$ set to zero showed no perceptible change in the rotational transform of the outermost flux surface. When in addition the $\ell=5$ amplitude was set to zero, so that only the $\ell=3$ and $\ell=4$ amplitudes remained, it was found that the rotational transform was decreased to 0.904. To summarize, the improvements obtained with the first order calculation discussed here are not very sensitive to perturbations of the harmonic amplitudes.

V. CONCLUSIONS AND DISCUSSION

The primary result of this paper is that one can dramatically improve the structure of the surfaces of typical vacuum magnetic fields by adding small vacuum perturbations to eliminate the island structure. However, there remain substantial questions of both mathematical and practical nature.

On the mathematical side, there remains the question of whether vacuum magnetic fields with rotational transform and dense nested toroidal flux surfaces but no internal currents truly exist. On the basis of this work, the author believes the answer to be positive. However, the construction of a mathematical proof would appear to be exceedingly difficult.

The answer to that question would bear on whether higher order calculations would be fruitful. Higher order corrections are conceptually straightforward to calculate. The result of first-order theory is a new vector potential for which the new flux function Ψ is an invariant to $\mathcal{O}(\varepsilon^2)$. These functions can be used as a starting point for a second-order calculation of the toroidal harmonics needed to cancel the resonances. However, higher order calculations can continue to be fruitful only if this method is convergent, for which it is necessary that a solution exist.

In any case there remains the practical question of how these methods might be used to design the coils for producing these magnetic fields. There do not appear to be any difficulties in principle. The averaging introduced in Sec. III can be applied to any arbitrary magnetic field. The perturbing fields of Sec. IV could be those produced by small changes in the coil winding law. However, such a

design procedure would involve extensive computer calculations in view of the absence of simple analytic formulas for the magnetic fields produced by moderately complicated coils. Moreover, it should be combined with other design techniques. As one example there is the work of Chodura et al.[16], in which magnetic fields are optimized with regard to the equilibrium β-limits.

A further question is whether these methods can be extended to calculate finite pressure equilibria. Indeed, even whether infinitesimal-pressure equilibria exist is an unanswered question. A vacuum field with nested toroidal flux surfaces has a nearby infinitesimal-pressure equilibrium only if the line integral $\oint d\ell/B$ has the same value for each of the closed lines on a surface with rational rotational transform.[17] It has not been shown that this must be true if a vacuum field has dense flux surfaces. On the other hand, no counterexample can be given in the absence of known exactly integrable vacuum fields.

VI. ACKNOWLEDGMENTS

The author would like to thank Marshall Rosenbluth, Robert Littlejohn, and John Greene for useful discussions during the course of this work.

This work was supported by the Office of Fusion Energy of the U.S. Department of Energy under contract DE FG05-80ET-53088.

Appendix A

Toroidal Coordinates

The toroidal coordinates used in this paper have been chosen with two objectives in mind. First, they must be equivalent to the coordinates introduced by Morse and Feshbach (Ref. 18, p. 1301), in which Laplace's equation separates. Second, the coordinates must adhere to the extent possible to established conventions.

The coordinates are shown in Fig. 1. The transformation law between the (ξ,η,ϕ) system and the cartesian coordinates is

$$\begin{aligned} X &= R_0(1-\xi^2)^{1/2}\cos\phi(1-\xi\cos\eta)^{-1} \\ Y &= R_0(1-\xi^2)^{1/2}\sin\phi(1-\xi\cos\eta)^{-1} \\ Z &= -R_0\xi\sin\eta(1-\xi\cos\eta)^{-1} . \end{aligned} \tag{A1}$$

The sign in the last transformation law has been chosen to allow both (R,ϕ,z), where $R = (X^2+Y^2)^{1/2}$, and (ξ,η,ϕ) to be right-handed orientations.

The inversion is obtained through the intermediate variable

$$\rho \equiv 2RR_0/(R_0^2+Z^2+R^2) . \tag{A3}$$

One finds

$$\xi = (1-\rho^2)^{1/2} \tag{A4}$$

and

$$\tan\eta = -\rho Z/(R-\rho R_0) \ . \tag{A5}$$

Constant-ξ surfaces are circular tori. The circles are centered at $R_c = R_0/\rho$ and have radius $r = R_0\xi/\rho$. Therefore these circles have inverse aspect ratio $r/R_c = \xi$.

These coordinates are orthogonal. Thus, the metric tensor is diagonal, $g_{ij} = h_i^2\delta_{ij}$. It has elements

$$h_\xi = R_0(1-\xi^2)^{-1/2}(1-\xi\cos\eta)^{-1} \ ,$$

$$h_\eta = R_0\xi(1-\xi\cos\eta)^{-1} \ ,$$

and

$$h_\phi = R_0(1-\xi^2)^{1/2}(1-\xi\cos\eta)^{-1} \ . \tag{A6}$$

The volume element for these coordinates is

$$J = \xi(1-\xi\cos\eta)^{-3} \ . \tag{A7}$$

Appendix B

Toroidal Magnetic Scalar Potential

The general scalar potential satisfying $\nabla^2\Psi = 0$, regular at $\xi=0$, and allowing for an axial current can be deduced from Ref. 18. It is

$$\Psi = I\phi + (1 - \xi \cos\eta)^{1/2} \sum_{\ell=-\infty}^{\infty} \sum_{m=-\infty}^{\infty} \alpha_{\ell m} U_{\ell m}(\xi) e^{i\ell\eta + im\phi} \qquad (B1)$$

where

$$U_{\ell m}(\xi) = \xi^{-1/2} Q^{|m|}_{\ell-1/2}(1/\xi) \, . \qquad (B2)$$

Throughout this work we will select units such that I=1. The complex coefficients $\alpha_{\ell m}$ are arbitrary provided $\alpha_{\ell,m} = \alpha^*_{-\ell,m}$. The function $Q^{\mu}_{\nu}(x)$ is the modified Legendre function of the second kind of order μ and degree ν.

The functions $U_{\ell m}(\xi)$ are analytic for $0 \leq |\xi| < 1$. Using Eq. (B2) and the known[19,20] properties of $Q^{\mu}_{\nu}(\alpha)$, one can derive several properties of $U_{\ell m}(\xi)$. First, $U_{\ell m}(\xi)$ satisfies the differential equation

$$\frac{d}{d\xi}\left[\xi(1-\xi^2)\frac{dU_{\ell m}}{d\xi}\right] = \left(\frac{3\xi}{4} + \frac{\ell^2}{\xi} + \frac{m^2\xi}{1-\xi^2}\right)U_{\ell m} \, . \qquad (B3)$$

Second, an integral representation is

$$U_{\ell m}(\xi) = \frac{(-1)^m \Gamma(\ell+m+1/2)}{2^{\ell+1/2}\Gamma(\ell+1/2)} \frac{\xi^{\ell}}{(1-\xi^2)^{m/2}} \int_0^{\pi} dt (\sin t)^{2\ell} (1+\xi\cos t)^{m-\ell-1/2} \, , \qquad (B4)$$

for $\ell \geq 0$ and $m \geq 0$. Third, derivatives may be obtained by the formula

$$\frac{dU_{\ell m}}{d\xi} = \frac{(\xi^2/2-\ell)U_{\ell m}/\xi + (\ell+m-1/2)U_{\ell-1,m}}{1-\xi^2} \cdot \tag{B5}$$

Fourth, one has the symmetry

$$U_{-\ell m} = U_{\ell m} \cdot \tag{B6}$$

Appendix C

Toroidal Magnetic Vector Potential

In this appendix we obtain the vector potential for the curl-free and divergence-free magnetic field obtained from the scalar potential (B1). The procedure in general coordinates, x^i, is as follows. From the scalar potential one obtains the covariant components of the magnetic field, $B_i = \partial\Psi/\partial x^i$. Application of the raising operation gives the contravariant components of the magnetic field, $B^j = g^{ji}B_i$. (Einstein summation notation is used in this appendix.) The magnetic 2-form is obtained from the covariant components by taking the dual, $B_{k\ell} = J[k\ell j]B^j$, where $[k\ell j]$ is the Levi-Civita symbol. Finally, the covariant components of the vector potential A must be chosen to satisfy $B_{k\ell} = \partial A_\ell/\partial x^k - \partial A_k/\partial x^\ell$. This last step is guaranteed to work because $\nabla\cdot B = 0$, i.e., the magnetic 2-form is closed. Also, this last step is arbitrary to within a gauge transformation.

The results of carrying out this procedure are:

1. Toroidal field

For $\Phi^T \equiv \phi$, (C1)

we find

$$A^T_\xi = 0$$

$$A^T_\eta = \frac{1}{2}\{(1-\cos\eta)^{-1}\ell n[(1-\xi\cos\eta)/(1-\xi)] + (1+\cos\eta)^{-1}\ell n[(1-\xi\cos\eta)/(1+\xi)]\},$$

and $A^T_\phi = 0$. (C2)

The result for A_η^T is not singular at $\eta=0,\pi$ in spite of its appearance.

2. Helical fields ($m\neq 0$).

For

$$\Phi^{\ell m} \equiv (1-\xi\ \cos\eta)^{1/2}\ U_{\ell m}(\xi)\exp(i\ell\eta+im\phi)\ , \tag{C3}$$

we find

$$A_\xi^{\ell m} = \left[m\xi(1-\xi\ \cos\eta)\right]^{-1}\ U_{\ell m}(\xi)\ \frac{\partial}{\partial\eta}\left[(1-\xi\ \cos\eta)^{1/2}\ \exp(i\ell\eta+im\phi)\right]\ ,$$

$$A_\eta^{\ell m} = i\left[m(1-\xi\ \cos\eta)\right]^{-1}\ \xi(1-\xi^2)\ \frac{\partial}{\partial\xi}\left[(1-\ \cos\eta)^{1/2}\ U_{\ell m}(\xi)\right]\exp(i\ell\eta+im\phi)\ ,$$

and $A_\phi^{\ell m} = 0$. (C4)

3. Vertical fields ($m=0$).

For the vertical field,

$$\Phi^{\ell 0} = (1-\xi\ \cos\eta)^{1/2}\ U_{\ell 0}(\xi)e^{i\ell\eta}\ , \tag{C5}$$

we find

$$A_\xi^{\ell 0} = 0\ ,$$

$$A_\eta^{\ell 0} = 0\ , \tag{C6}$$

and

$$A_\phi^{\ell 0} = -\int_0^\xi dx\left[x(1-x\ \cos\eta)\right]^{-1}\ U_{\ell 0}(x)\ \frac{\partial}{\partial\eta}\left[(1-x\ \cos\eta)^{1/2}\ \exp(i\ell\eta)\right]\ .$$

Appendix D

Averaged Vector Potentials

The development of the text requires the solution of the following problem. Given a particular vector potential A, and a particular helical angle $h \equiv \ell_0\eta + n_0\phi$, find the averaged vector potential, which has components defined by

$$\bar{A}_i \equiv \frac{1}{2\pi}\int_0^{2\pi} d\eta\, A_i(\xi,\eta,\phi = (h-\ell_0\eta)/m_0) \ . \tag{D1}$$

In the integration (D1) the variables ξ and h are held fixed.

For the purpose of this paper we need the average of only A^T and $A^{\ell_0 m_0}$. The results for the toroidal field are

$$\bar{A}^T_\xi = 0 \ ,$$

$$\bar{A}^T_\eta = (1-\xi^2)^{-1/2} - 1 \ , \tag{D2}$$

and $$\bar{A}^T_\phi = 0 \ .$$

The results for the appropriate helical field are

$$\bar{A}^{\ell_0 m_0}_\xi = \sqrt{2}\ \ell_0(\pi m_0 \xi)^{-1}\ U_{\ell_0 m_0}(\xi) U_{00}(\xi)\exp(ih) \ ,$$

$$\bar{A}^{\ell_0 m_0}_\eta = i\sqrt{2}\ (\pi m_0)^{-1}\xi(1-\xi^2)\ \left[\frac{dU_{\ell_0 m_0}}{d\xi}\ U_{00} - \frac{dU_{00}}{d\xi}\ U_{\ell_0 m_0}\right]\exp(ih) \ , \tag{D3}$$

and $\bar{A}^{\ell_0 m_0}_\phi = 0$.

References

1. M. D. Kruskal and R. M. Kulsrud, Phys. Fluids 1, 265(1958).

2. H. Grad, Phys. Fluids 10, 137(1967).

3. L. Spitzer, Phys. Fluids 1, 253(1958).

4. K. Miyamoto, Nucl. Fusion 18, 243(1978).

5. R. M. Sinclair, J. C Hosea, and G. V. Sheffield, Rev. Sci. Inst. 41, 1552(1970).

6. J. A. Rome, J. H. Harris, and B. F. Masden, Bull. Am. Phys. Soc. 27, 1021(1982).

7. D. T. Anderson, J. A. Derr, and J. L. Shohet, IEEE Trans. Plasma Sci., PS-9, 212(1981).

8. R. G. Littlejohn, J. Math. Phys. 23, 742(1982).

9. R. G. Littlejohn and J. R. Cary, Ann. Phys. (NY), to be published (1983).

10. J. R. Cary, Phys. Rev. Lett. 49, 276(1983).

11. C. F. F. Karney, Physica D, to be published (1983).

12. B. V. Chirikov, Phys. Rep. 52, 263(1979).

13. J. M. Greene and J. L. Johnson, Phys. Fluids 4, 875(1961).

14. R. Pexton, Lawrence Livermore National Laboratory (private communication).

15. J. Sedlak, University of Texas at Austin (private communication).

16. R. Chodura, W. Dommaschk, W. Lotz, J. Nührenberg, and A. Schlüter, in Plasma Physics and Controlled Nuclear Fusion Research (International Atomic Energy Agency, Vienna, 1980), Vol. I, p. 807.

17. W. A. Newcomb, Phys. Fluids 2, 362(1959).

18. P. M. Morse and H. Feshbach, Methods of Theoretical Physics (McGraw-Hill, New York, 1953).

19. I. A. Stegun in Handbook of Mathematical Functions (Dover, New York, 1968) p. 336.

20. Higher Transcendental Functions, A. Erdelyi, ed. (McGraw-Hill, New York, 1953) Ch. III.

Figure Captions

Fig. 1 -

Coordinates used in this paper.

Fig. 2 -

Surface of section for $\mathrm{Re}(\alpha_{3,7}) = -7 \times 10^{-5}$ and $\mathrm{Im}(\alpha_{3,7}) = 0$.

Fig. 3 -

Surface of section for $\mathrm{Re}(\alpha_{3,7}) = -3.5 \times 10^{-5}$ and $\mathrm{Im}(\alpha_{3,7}) = 0$.

Fig. 4 -

Surface of section for $\mathrm{Re}(\alpha_{3,7}) = -1 \times 10^{-5}$ and $\mathrm{Im}(\alpha_{3,7}) = 0$.

Fig. 5 -

Comparison of surface of section with the invariant obtained by averaging for the case of Fig. 3.

Fig. 6 -

Comparison of surface of section with the invariant obtained by averaging for the case of Fig. 4.

Fig. 7 -

Rotational transform for the averaged fields of the case of Fig. 3.

Fig. 8 -

Surface of section for the parameters of Table II.

Table Captions

Table I -

Resonance locations and widths for the case of Fig. 3.

Table II -

Field amplitudes needed to cancel resonance amplitudes for the case of Fig. 3.

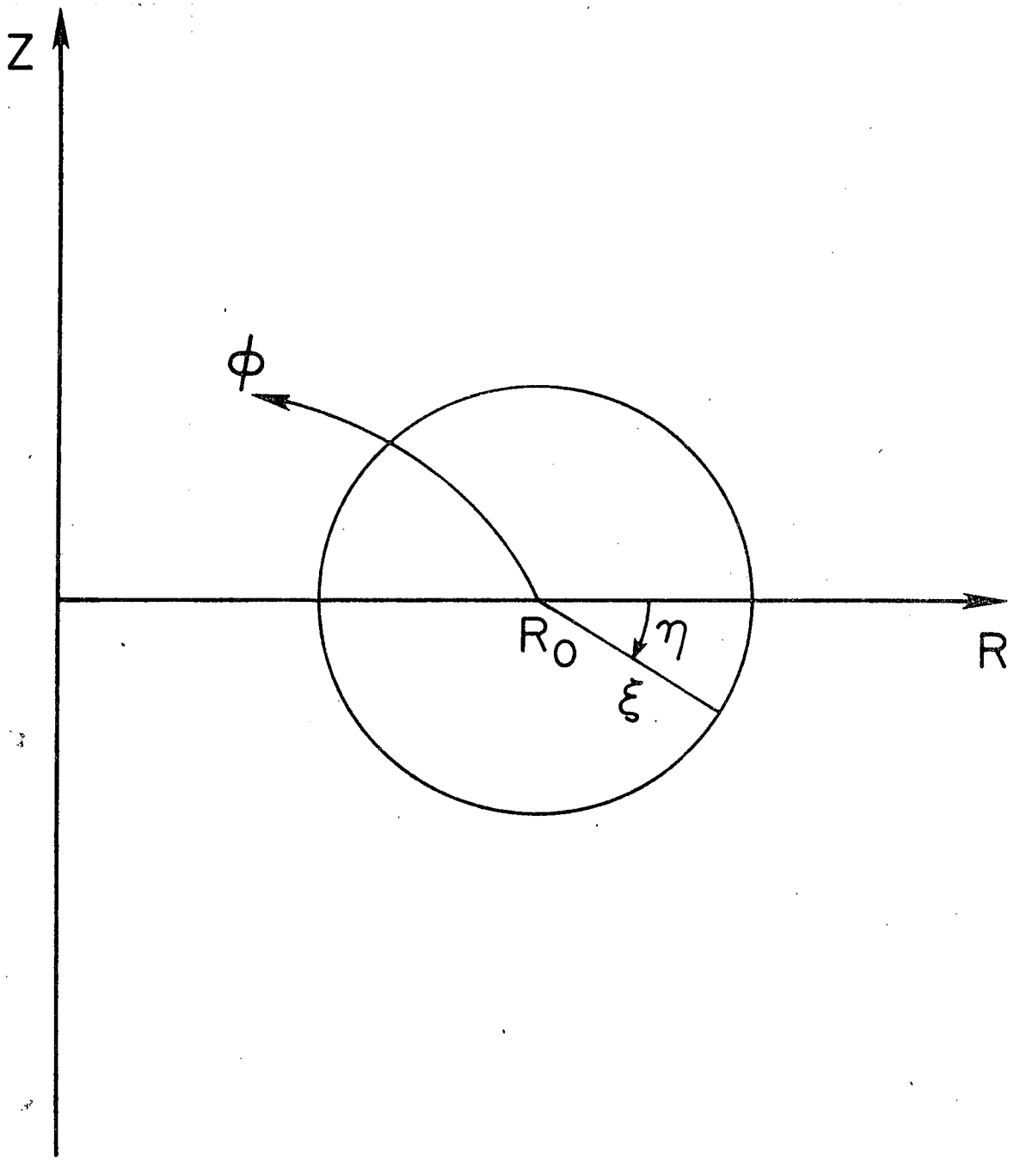

FIG. 1

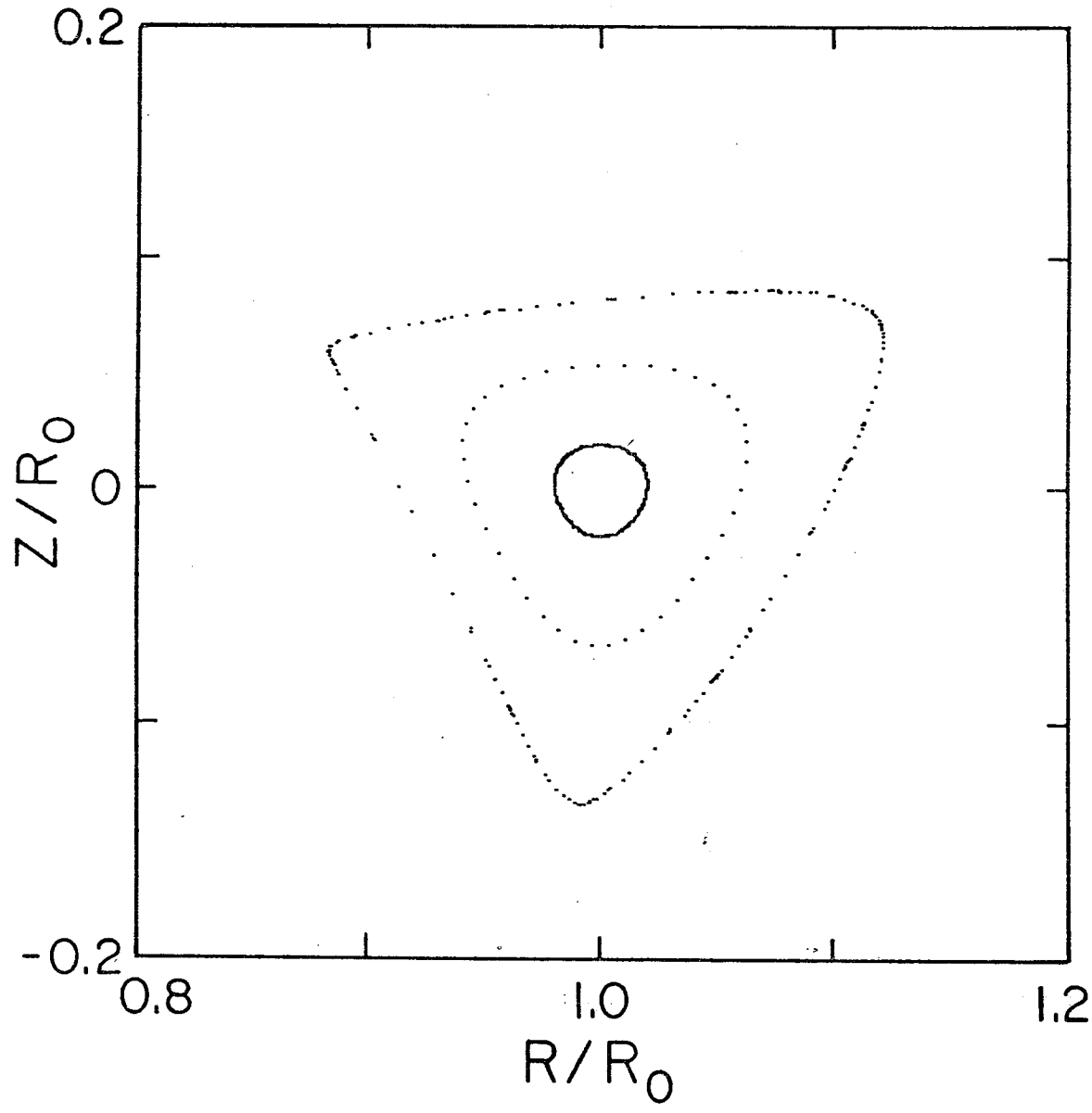

FIG. 2

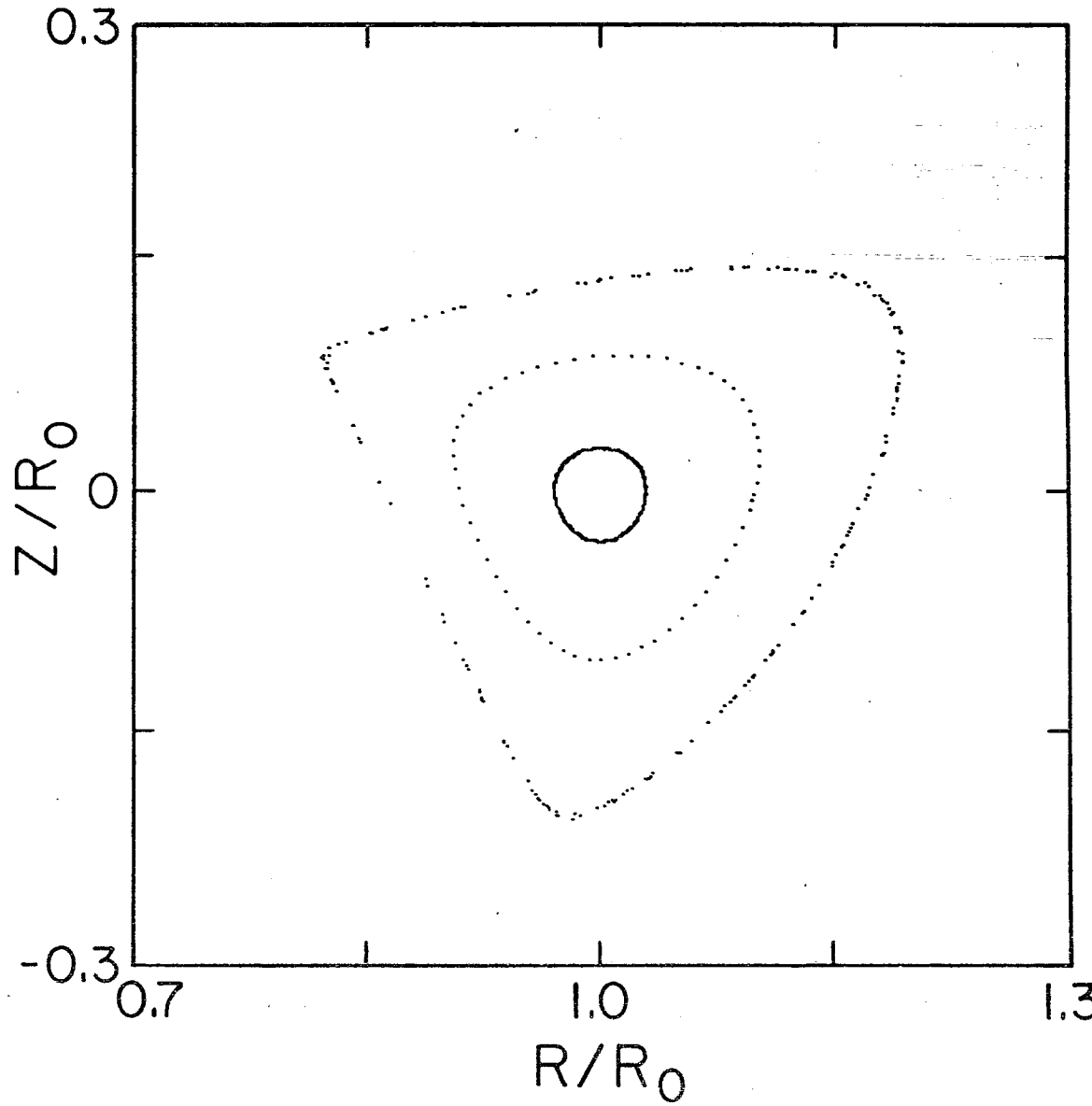

FIG. 3

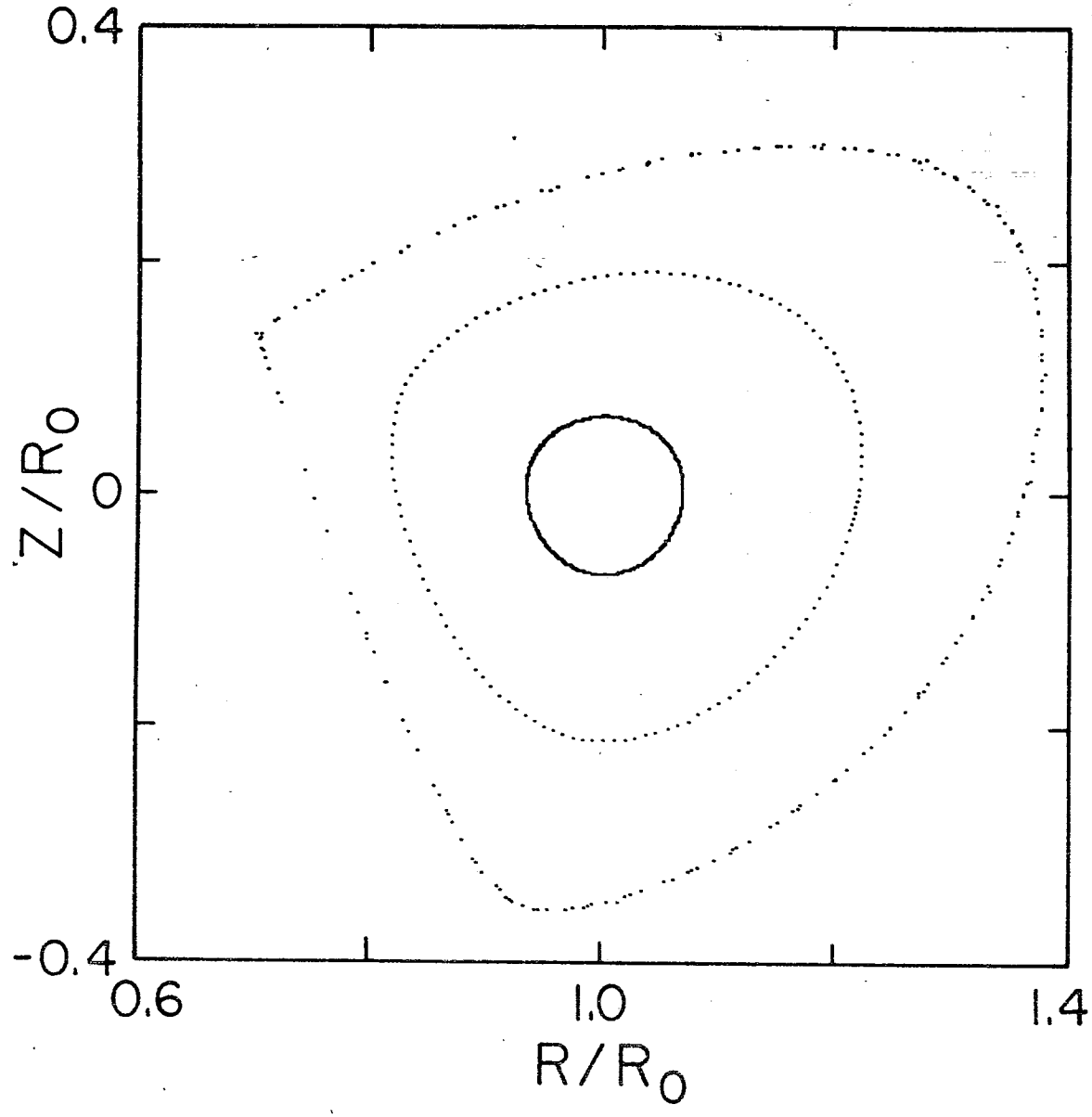

FIG. 4

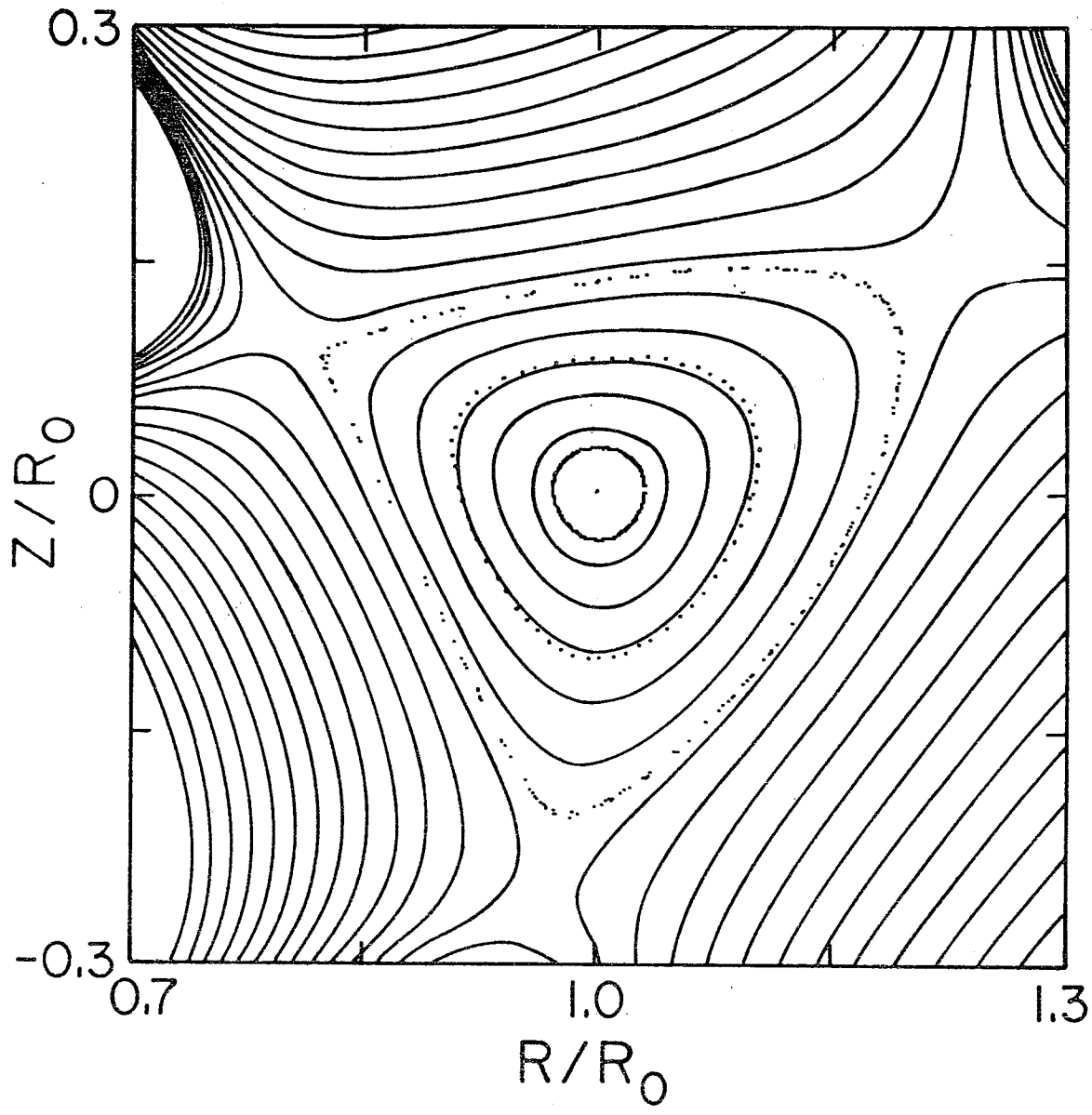

FIG. 5

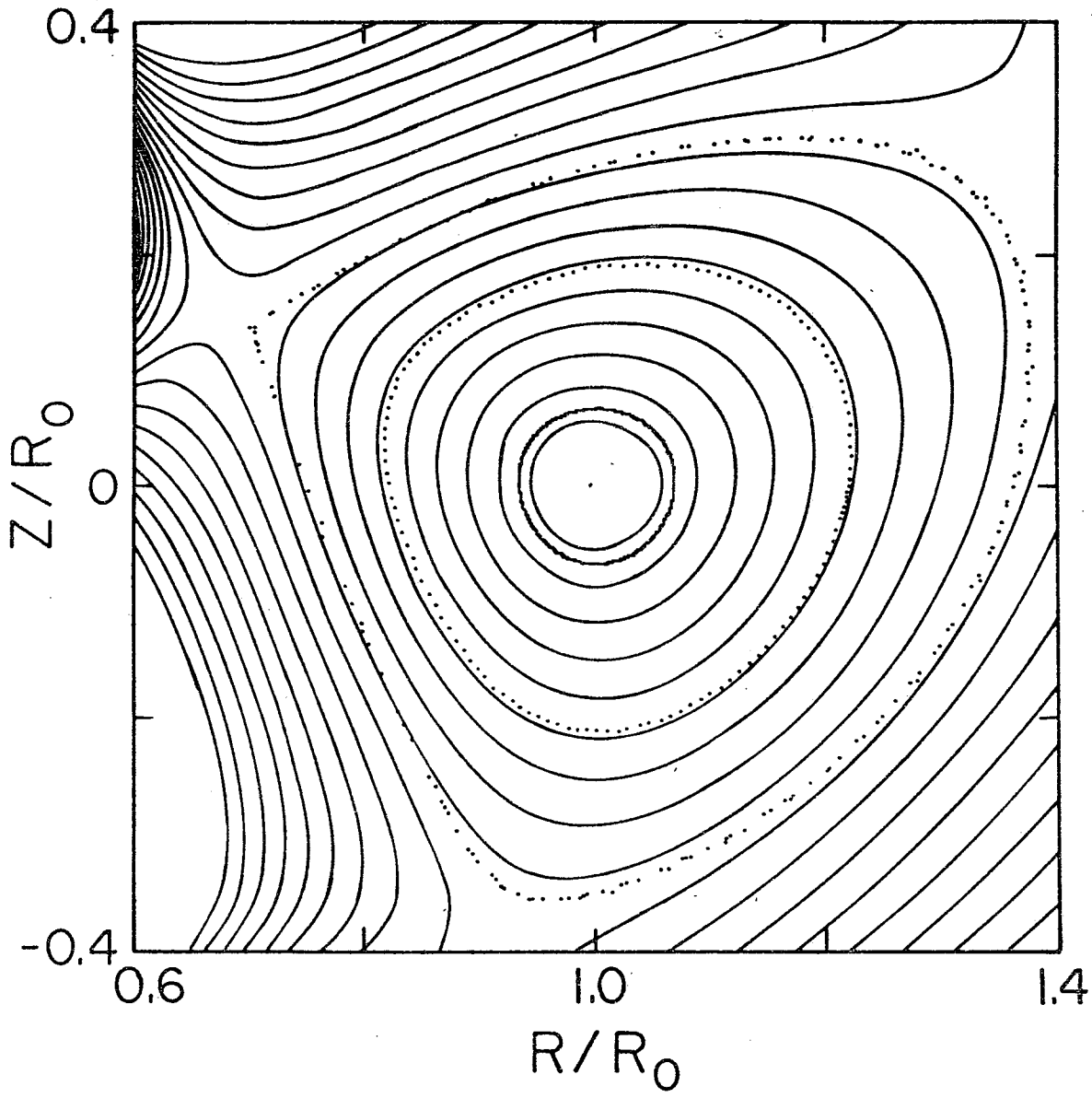

FIG. 6

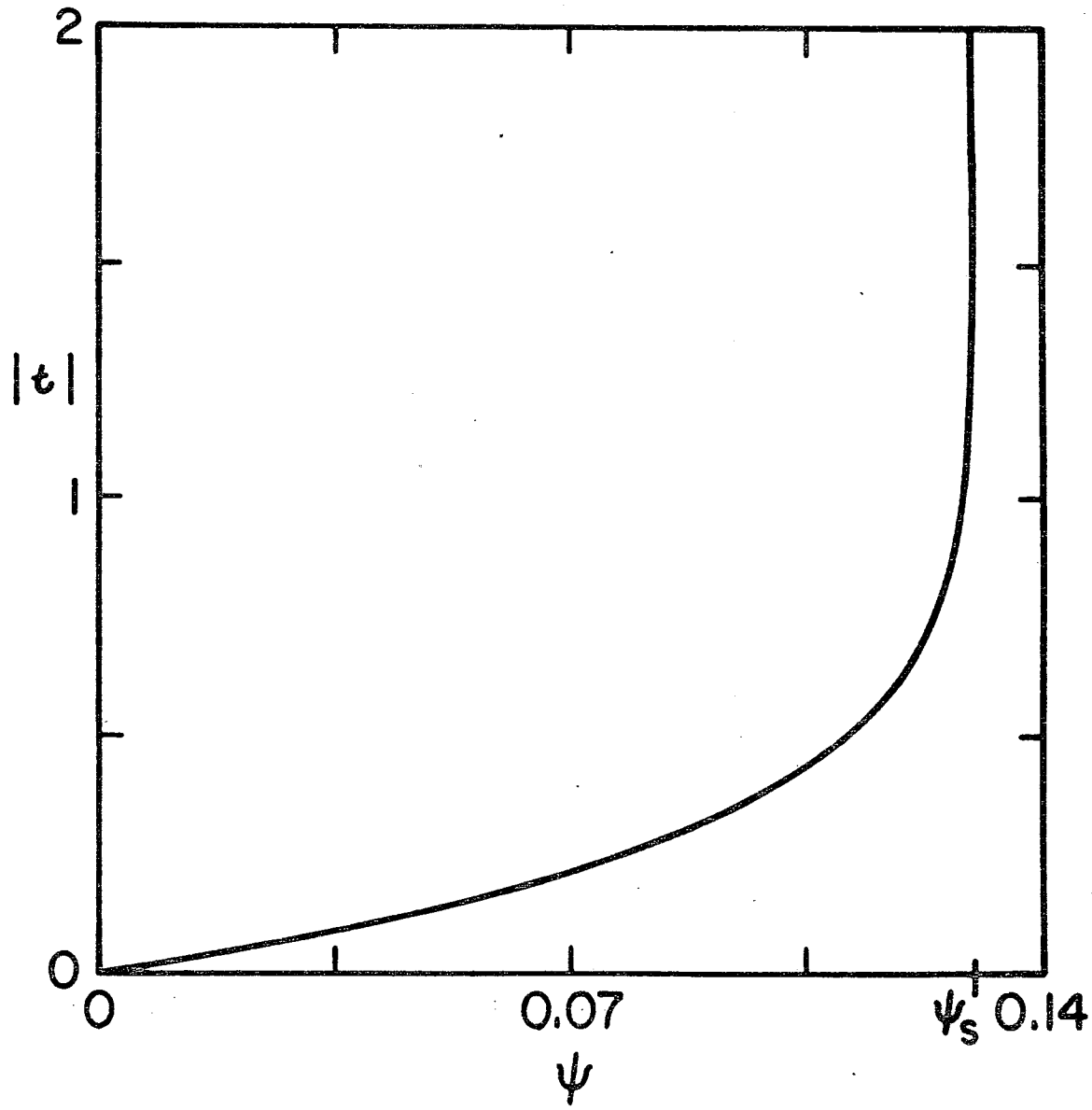

FIG. 7

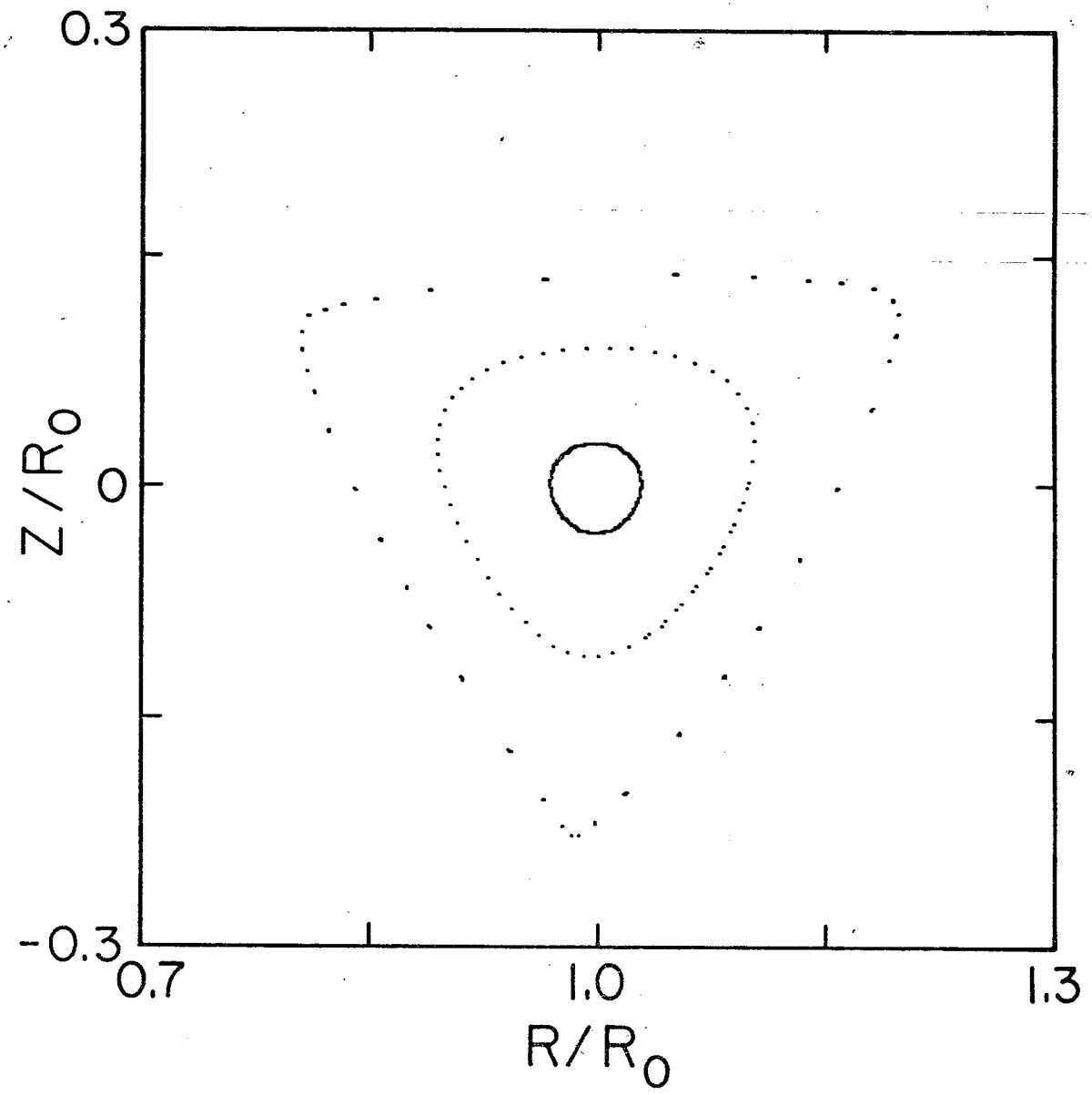

FIG. 8

j	k	t	ψ_{jk}	$\Delta\psi_{jk}$
1	1	1.75	0.0129532	1.1×10^{-6}
2	1	1.40	0.0129521	3.41×10^{-5}
3	1	1.17	0.0129324	4.31×10^{-5}
7	2	1.08	0.0129044	4.0×10^{-7}
4	1	1.00	0.0128604	2.51×10^{-5}
9	2	0.93	0.0127996	5.0×10^{-8}
5	1	0.88	0.0127229	1.06×10^{-5}

TABLE I

ℓ	m	$Re(\alpha_{\ell,m})$	$Im(\alpha_{\ell,m})$
3	7	-3.5×10^{-5}	0.0
4	7	-2.243×10^{-5}	3.56×10^{-7}
5	7	-3.458×10^{-6}	-5.4×10^{-8}
6	7	-1.246×10^{-6}	-3.0×10^{-9}
7	7	-5.51×10^{-7}	0.0
8	7	-2.74×10^{-7}	0.0
9	7	-1.47×10^{-7}	0.0
10	7	-8.3×10^{-8}	0.0

TABLE II